
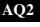


2 **Carrageenan-based superabsorbent biopolymers mitigate**
3 **autogenous shrinkage in ordinary portland cement**

4 Anastasia N. Aday · Jorge Osio-Norgaard · Kyle E. O. Foster · Wil V. Srubar III 

5 Received: 8 December 2017 / Accepted: 13 February 2018
6 © RILEM 2018

7 **Abstract** We report the synthesis and characteriza-
8 tion of biobased superabsorbent copolymers from κ-
9 carrageenan and poly(acrylic acid) that mitigate
10 autogenous shrinkage in ordinary portland cement
11 paste. Synthesized via free radical graft polymeriza-
12 tion, the biobased superabsorbent polymers (SAPs)
13 were characterized with regard to their thermochem-
14 ical properties and swelling behavior in both aqueous
15  and ionic solutions. The biobased SAPs were incor-
16 porated into cement paste to investigate their ability to
17 mitigate autogenous shrinkage cracking in high-per-
18 formance concrete. Results demonstrate that the
19 biobased SAPs absorb up to 438 and 94 [g/g] (by
20 mass) in aqueous and ionic solutions, respectively,
21 after 24 h. Furthermore, the biobased SAPs were
22 successful in mitigating shrinkage in low water-to-
23 cement ratio pastes. While the control paste exhibited
24 negative strain and ultimate shrinkage cracking, the
25 samples containing biobased SAP experienced net-
26  positive expansion during cement hydration.

Keywords Superabsorbent polymer (SAP) · Internal 27
curing · Biopolymers · Cement · Autogenous 28
shrinkage 29

1 Introduction 30

1.1 Superabsorbent polymers 31

Over the past few decades, the use of superabsorbent 32
polymers (SAPs) in cement-based materials has 33
increased due to their proven ability to improve initial 34
and long-term performance. SAPs have been shown to 35
mitigate early-age autogenous shrinkage [1, 2], 36
increase freeze–thaw resistance [3–5], and, more 37
recently, to impart self-healing characteristics [6, 7] 38
to ordinary portland cement (OPC) concrete. While a 39
majority of these studies employ commercially avail- 40
able SAPs, some studies have reported the synthesis 41
and chemical characterization of novel SAPs [8–10] 42
and their interaction with cement-based materials. 43

SAPs are crosslinked networks of ultra-hydrophilic 44
polymers that can absorb up to 100,000% of their dry 45
weight in aqueous solutions [11]. The ability of the 46
polymer to absorb fluids is attributed to the abundance 47
of hydrophilic functional groups present on the 48
polymer backbone, while the crosslinks in SAP 49
networks render the polymer insoluble [12, 13]. While 50
commonplace SAPs have been synthesized using ionic 51

A1 A. N. Aday · K. E. O. Foster · W. V. Srubar III (✉)
A2 Materials Science and Engineering Program, University
A3 of Colorado Boulder, ECOT 441 UCB 428, Boulder,
A4 CO 80309-0428, USA
A5 e-mail: wsrubar@colorado.edu

A6 J. Osio-Norgaard · W. V. Srubar III
A7 Department of Civil, Environmental, and Architectural
A8 Engineering, University of Colorado Boulder, ECOT 441
A9 UCB 428, Boulder, CO 80309-0428, USA

acrylate/acrylamide homopolymers, the use of super-absorbent hydrophilic biopolymers, such as alginates, celluloses, and carrageenans [14], as biological precursors for SAPs has been largely unexplored for applications in cementitious materials.

1.2 Carrageenan

Carrageenans are a class of linear, hydrophilic polysaccharides present in various species of red seaweeds in the class, *Rhodophyceae*. Carrageenans are classified using Greek prefixes, such as κ , ι , and λ . All κ , ι , and λ carrageenans consist primarily of sulfated esters (i.e., D-galactose and 3,6-anhydro-D-galactose copolymers) with α -1,3 and β -1,4 linkages [15]. Carrageenans are typically extracted through an alkaline process, resulting in a negatively charged polymer with a corresponding cation of either Na^+ or K^+ [16, 17]. Carrageenans are categorized per the location and number of these sulfate ester groups, with κ , ι , and λ carrageenans having one, two, and three groups, respectively [18]. Of these carrageenans, κ -carrageenan (Fig. 1) and ι -carrageenan both swell and form gels in the presence of K^+ and Ca^{2+} ions [15]. While the gelling behavior of κ -carrageenan is complex, the gels have a double helix conformation in the cooled state, creating a strong and brittle gel with thermoreversible gelling properties in water [19, 20].

1.3 Autogenous shrinkage

Autogenous shrinkage (AS) is a ubiquitous early-age issue with concrete, particularly high-performance (i.e., high strength, low water-to-cement (w/c) ratio) pastes, mortars, and concrete [21–23]. AS is a phenomenon caused by self-desiccation of cement paste as it pulls water from the surface of calcium silicate hydrate (C–S–H) gel to further the hydration of anhydrous cement [21]. Self-desiccation creates internal stresses leading to cracking in the paste, which can

diminish mechanical properties and long-term durability [21].

Internal curing methodologies have been proposed to address AS [24]. Internal curing approaches have utilized SAPs, pre-wetted lightweight aggregates, or other admixtures to provide additional entrained water to anhydrous cement. The additional water reduces early-age compressive strength without compromising overall strength [23, 25]. For internal curing using SAPs, dry SAPs are mixed in with the cement and absorb additional water stipulated by the mix design. As the initially hydrated cement begins to undergo self-desiccation, these SAPs release absorbed water to compensate for moisture loss, thus mitigating shrinkage and potential crack formation. Ongoing work has recently established procedural methods that describe characterization of SAP sorption properties prior to usage in cement-based materials, thus aiding in the understanding of how SAPs can be utilized to mitigate AS [26, 27].

1.4 Scope of work

The objective of this work was to synthesize and characterize a superabsorbent, biobased copolymer from κ -carrageenan and poly(acrylic acid), adhering to green chemistry practices with an aqueous, free radical copolymerization technique. Biobased SAPs are synthesized herein from an acrylic acid monomer covalently crosslinked with a multivalent agent (*N,N'*-methylenebisacrylamide) in a free radical polymerization that grafts the poly(acrylic acid) chain to κ -carrageenan. The polymerization process in this study proceeds in an aqueous media due to the solubility of the biopolymer, monomer, and crosslinking agent. After thermochemical and physical swelling characterization, the resulting synthesized SAPs were tested as a water-retention additive in cement paste to evaluate their effectiveness in reducing autogenous shrinkage.

D-galactose-4-sulphate 3,6-anhydro-D-galactose

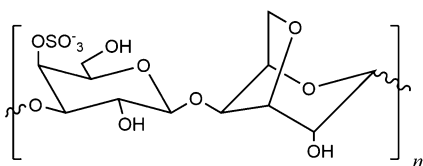


Fig. 1 Chemical structure of κ -carrageenan [17]

2 Materials and methods

2.1 Materials

κ -Carrageenan (κ C), acrylic acid (AA), *N,N'*-methylenebisacrylamide (MBA), ammonium persulfate (APS), and sodium hydroxide (NaOH) were

Author Proof



131 obtained from Sigma-Aldrich and used without further
132 purification. A stock solution of 1 M NaOH was
133 prepared. The cement used in this study was a
134 commercially available Type I/II OPC (Quikrete[®])
135 that complies with ASTM C150. See Table 1 for
136 chemical composition of OPC obtained via induc-
137 tively coupled plasma optical emission spectroscopy
138 (ICP-OES).

139 2.2 Methods

140 2.2.1 Biobased SAP synthesis

141 The biobased SAPs were synthesized using free
142 radical graft polymerization under ambient conditions.
143 Deionized water was added to a beaker and heated to
144 70 °C in an oil bath. κC was continuously added and
145 stirred with a stir bar at 300 rpm until a homogeneous
146 solution was achieved. To the solution, AA was added
147 followed by MBA with continuous stirring. The water-
148 soluble initiator, APS, was added to the solution and
149 stirred until the viscosity increased to the point of gel
150 formation. The gel was then removed from the oil bath
151 and allowed to cool under ambient conditions. Upon
152 cooling, a 1 M solution of NaOH was added to the gel
153 to neutralize the carboxylic acid groups and hand-
154 stirred until the gel had absorbed the solution. The gel
155 was then transferred to a beaker of methanol to
156 dewater for 1 h. The methanol was decanted and fresh
157 methanol was added to the gel to dewater for 24 h.
158 After dewatering, the gel was allowed to dry in an
159 oven (20% ± 5% RH, 40 °C ± 5 °C). Dried gel was
160 then ground into a powder using a mechanical grinder
161 and sieved to a 125–250 μm particle size. Dried
162 samples were then stored away from heat, light, and
163 moisture. To minimize variables in the synthesis, only
164 the amount of AA monomer was varied in order to
165 investigate the swelling behavior at various AA
166 concentrations. Figure 2 illustrates a generalized
167 mechanism of the grafting and crosslinking of κC
168 onto acrylic acid. The APS initiator thermally decom-
169 poses to generate a sulfate anion-radical, where the

radical abstracts hydrogen from the hydroxyl group of
κC forming an alkoxy radical (APS-κC). Active
centers on the APS-κC redox system then radically
initiate the polymerization of AA resulting in a graft
copolymer. See Table 2 for a list of sample
formulations.

2.2.2 Physical and chemical characterization

2.2.2.1 *Differential scanning calorimetry* Thermal
data for samples dried for at least 3 days were
collected using a TA Instruments Q2000 Differential
Scanning Calorimeter (DSC) in a N₂ environment
using a purge rate of 50 mL/min. 6 mg samples of
SAP were placed in hermetically sealed aluminum
pans. The samples were first equilibrated to 15 °C
followed by heating at a rate of 10 °C/min to 250 °C.
The samples were then cooled at a rate of 10 °C/min to
0 °C and then heated again to 250 °C at a rate of
10 °C/min. Enthalpy calculations and transition
temperatures were analyzed using Universal
Analysis software (TA Instruments).

2.2.2.2 *Thermogravimetric analysis* Thermogravi-
metric analysis (TGA) of dried SAPs was performed
using a TA Q50 TGA. All samples were tested under
nitrogen gas. All samples underwent the same
sequence of thermal processing: equilibration at
25 °C for 1 min, followed by heating at a rate of
10 °C/min to 900 °C where they were held for 5 min,
then cooled rapidly back to 25 °C. All weight-percent
traces were differentiated with respect to time in
Origin 2017 analysis software to emphasize major
decomposition events of each material.

2.2.2.3 *Fourier transform infrared spectroscopy* Fourier Transform Infrared Spectroscopy (FTIR) was conducted using a Cary 630 equipped with an Attenuated Total Reflection (ATR) accessory. 40 spectra were collected from 4000 to 500 cm⁻¹ at a resolution of 1 cm⁻¹ for each sample. All spectra were processed using Origin 2017 analysis software.

Table 1 Chemical composition of Type I/II OPC

Chemical composition (wt%)	CaO	SiO ₂	Al ₂ O ₃	Fe ₂ O ₃	K ₂ O	Na ₂ O	MgO	Other
Type I/II Cement	73.7	12	7	4.1	0.9	0.3	0.0003	2



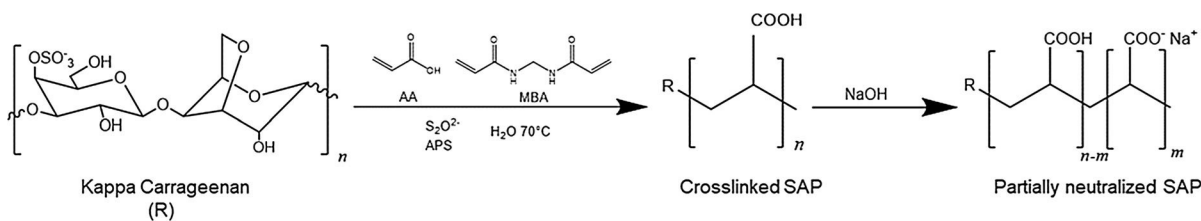


Fig. 2 Generalized mechanism of the synthesis of biobased SAP

Table 2 Biobased SAP sample compositions

Sample	κC (g)	AA (mL)	MBA (g)	APS (g)
SAP A	1.00	3.5	0.1	0.2
SAP B	1.00	2.5	0.1	0.2

208 2.2.2.4 Scanning electron microscopy Scanning
 209 electron microscopy (SEM, JEOL JSM-6840LV)
 210 was performed using an accelerating voltage of
 211 15 kV to confirm particle size and analyze polymer
 212 morphology. Non-powdered and powdered samples
 213 were attached to aluminum stubs using carbon tape
 214 and then sputter-coated with Au (Cressington
 215 108auto) for 20–25 s at mA (~ 3.5–4.0 nm) in an
 216 Ar-rich environment.

217 2.2.2.5 Physical swelling All dried samples were
 218 weighed and added to a pre-wetted, 150 μm mesh bag,
 219 immersed in deionized water, tap water, 0.1 M NaOH
 220 solution, and a synthetic pore solution at room
 221 temperature, and allowed to swell in time intervals
 222 of 1, 3, 5, 10, 15, 30, 60, 120 min, and 24 h. During the
 223 swelling tests, no SAP particle loss to the solution was
 224 observed. A synthetic concrete pore solution (pH 13.4)
 225 was synthesized to mimic the solution chemistry that
 226 is typically observed during OPC hydration reactions.
 227 The solution was saturated with Ca(OH)₂, 11.22 g/L
 228 KOH, 4.0 g/L NaOH, 13.77 g/L Ca(SO₂)₄ were added
 229 to 1 L of deionized water, where the measured ion
 230 composition can be obtained from Ghods et al. [28].
 231 Swelling ratio (*Q*) was measured by removing the bag
 232 from the solution and excess solution was allowed to
 233 drain from the bag. After correcting for solution
 234 absorbed by the bag, *Q* was calculated according to:

$$Q \left(\frac{g}{g} \right) = \frac{w_{wet} - w_{dry}}{w_{dry}} \quad (1)$$

236 where *w_{wet}* and *w_{dry}* are the weights of the moistened
 237 polymer and dry polymer, respectively.

2.2.3 Autogenous shrinkage

238

2.2.3.1 Cement paste preparation Similar to other
 239 studies [29–31], three samples of cement paste with a
 240 base w/c ratio of 0.30 and an entrained water content
 241 of 0.05 were prepared. The entrained water amount of
 242 0.05 is additional external water that is available for
 243 absorption by the SAPs to be supplied during cement
 244 hydration. From a hydration standpoint, a cement
 245 paste with a w/c ratio of 0.35 is identical to a cement
 246 paste with a base w/c ratio of 0.30 and an entrained w/c
 247 of 0.05 [23]. Table 3 lists the mixture design
 248 proportions of the paste samples.

239

240

241

242

243

244

245

246

247

248

249

All SAPs were added dry at 0.3% by weight of dry
 250 cement and pre-mixed into the cement for a homoge-
 251 nously distributed mixture. Water was added slowly
 252 during the first minute of mixing, and the pastes were
 253 mixed using a combination of mechanical and hand
 254 mixing for a total of time of 8 min.

250

251

252

253

254

255

2.2.3.2 Workability of paste A miniature slump
 256 cone was fabricated according to [32] to test the
 257 workability of the paste. The cone had a height of
 258 57 mm, with a top and bottom diameter of 19 mm and
 259 38 mm, respectively. Cement paste was added in
 260 increments and consolidated (i.e., tamped) in three
 261 layers. Slump was defined as the difference between
 262 the original height of the miniature slump cone and the
 263 height of the paste sample once the cone was removed
 264 from the fresh paste.

256

257

258

259

260

261

262

263

264

265

2.2.3.3 Time of set Time of set was conducted
 266 according to ASTM C191 with no modifications.
 267 The time-of-set specimens were stored in a moist
 268 chamber (90% ± 5% RH, 16 °C ± 2 °C). During the
 269 first half-hour of the test, measurements were taken
 270 after the rest period in ambient laboratory conditions.
 271 Final time of set was determined once the needle left
 272 no circular impression.

266

267

268

269

270

271

272

273



Author Proof

Table 3 Sample compositions for autogenous shrinkage testing

Sample	Base w/c	Entrained w/c	Cement (g)	SAP (g)
1 (Control)	0.35	–	460	–
2 (SAP A)	0.30	0.05	460	1.38
3 (SAP B)	0.30	0.05	460	1.38

274 2.2.3.4 *Autogenous shrinkage strain* Autogenous
 275 shrinkage testing was conducted according to ASTM
 276 C1698. The autogenous shrinkage device was
 277 fabricated in-house from rigid poly(vinyl chloride)
 278 (PVC) tubing for the supporting base and corrugated
 279 tubing for the sample molds. The rigidity of the PVC
 280 tubing utilized herein complies with ASTM D1785.
 281 Measurements were recorded every 30 min beginning
 282 at the time of final set (Day 0) for the first three hours.
 283 Subsequent measurements were taken on days 1, 2, 3,
 284 7, 14, and 28 for all specimens. All specimens were
 285 tested in duplicate.

286 3 Results

287 3.1 Physical swelling

288 Figure 3 shows the time-dependent swelling of
 289 biobased SAP samples in all aqueous and ionic
 290 solutions investigated herein. Both SAPs exhibit an
 291 initially accelerated increase in absorption in both
 292 aqueous and ionic solutions. The rate of swelling
 293 decreases after 60 min for all SAP samples. Table 4

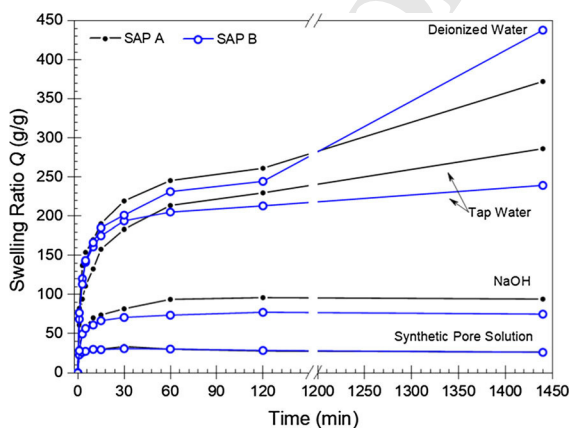


Fig. 3 Swelling ratio (Q) of biobased SAPs in aqueous and ionic solutions

294 lists the swelling ratio (Q) measurements for all
 295 samples swollen in aqueous and ionic solutions at 120
 296 min. The values represent the average of the highest
 297 swelling values from three solution absorbency trials.

298 All samples swollen in aqueous solutions achieved
 299 equilibrium swelling after 24 h, whereas SAP samples
 300 swollen in 0.1 M NaOH solution and the synthetic
 301 pore solution achieved equilibrium after 60 min and
 302 remained at equilibrium for the duration of the test
 303 period. SAPs swollen in deionized water exhibited the
 304 highest equilibrium swelling compared to SAPs
 305 swollen in all other solutions. SAP A achieved the
 306 highest average overall swelling performance in
 307 aqueous and NaOH solutions, while there was no
 308 statistical difference in the swelling performances
 309 between SAP A and SAP B in the synthetic pore
 310 solution. In comparison to non-biobased, poly(acrylic
 311 acid) SAPs [8, 29, 33] the Q ratios of SAPs A and B are
 312 comparatively larger. Previously reported swelling
 313 behavior of SAP samples of similar composition to
 314 SAP A and SAP B achieved swelling ratios in
 315 deionized water equal to 56.9 [g/g] and 170.5 [g/g].
 316 Thus, SAP A and SAP B exhibited relative increases in
 317 swelling ratios compared to these SAPs of 330.1% and
 318 53.3%, respectively [33]. For swelling ratios of non-
 319 biobased, poly(acrylic acid) SAPs in aqueous and Na^+
 320 solutions, Zhu et al. [8] reports Q values as high as 89
 321 [g/g] in deionized water and 47.5 [g/g] in a sodium
 322 chloride solution. Krafcik et al. [29] reports Q values
 323 of similar SAPs as high as 75 [g/g] and SAPs with high
 324 poly(acrylic acid content) up to 94 [g/g] in deionized
 325 water.

326 3.2 DSC

327 The DSC thermograms for the biobased SAPs, shown
 328 in Fig. 4, confirm no major thermal transitions within
 329 temperature ranges typical of cement hydration (20 to
 330 65 °C). The first transition at approximately 70 °C is a
 331 glass transition, T_g , of the SAP imparted by AA [34].



Table 4 Swelling ratio (Q) of SAPs in solution [g/g] at 120 min measurements

Sample	DI	Tap	0.1 M NaOH	Synthetic pore solution
SAP A	261.5 ± 59.3	230.0 ± 59.1	96.2 ± 22.0	27.9 ± 3.7
SAP B	244.7 ± 57.5	213.3 ± 48.6	77.4 ± 16.0	28.3 ± 2.6

Due to the proportion of AA to κC in the SAPs, the T_g is shifted higher than would be seen in κC alone. Previous studies have either reported no T_g behavior or a T_g near 45 °C for κC, depending on water content and the sensitivity of the equipment [35, 36]. The second transition peak near 155 °C is due to the vaporization of tightly bound water in κC [35, 37]. The third transition peak located around 202 °C is attributed to (1) the onset of the degradation of κC in the copolymer matrix and (2) the increase in anhydride content of the AA portion of the SAP, since this transition has been observed in crosslinked poly(acrylic acid) [34, 38]. Anhydride formation is further supported by the chemical stability of anhydrous compounds, which are observable only through the first heating cycle [39] provided no degradation occurs. Upon cooling and second heating, no additional thermal transition peaks other than those previously identified were observed (data not shown).

3.3 TGA

The TGA traces with the accompanying first derivative (DTG) curves are shown in Fig. 5 for the two biobased SAPs and the individual constituent materials, κC and poly(acrylic acid). The decomposition of each material proceeds to final weight percentages of 9.4, 12.6, 16.8, and 4.0% for SAP A, SAP B, κC, and crosslinked poly(acrylic acid), respectively. SAP A had a lower final weight percent compared to SAP B due to the higher proportion of AA in SAP A.

In the DTG curves, the degradation kinetics for both biobased SAPs follow similar trends with five main decomposition events represented by peaks of varying intensity. These five decomposition events are discussed individually from left to right in relation to the constituent material below. The first transition in the biobased SAPs around 270 °C are primarily attributable to the κC, with some influence from the AA. κC exhibits a sharp decrease in mass from 240 to 260 °C, which is stabilized in the biobased SAPs due to increased crosslinking density. The second and third transition in the biobased SAPs around 370 and 440 °C, respectively, can be attributed to the major decomposition of AA. The fourth transition around 700 °C aligns with the final major degradation event in κC. The fifth transition around 780 °C is similarly located to the final degradation event in AA.

Overall, the thermal traces demonstrate thermal stability for these polymers for internal curing applications in cement paste, mortar, and concrete. Thermal stability (> 90% weight) is retained at 200 °C prior to any degradation events, which, as noted, is well above typical hydration temperatures for cement-based materials.

3.4 SEM

Figure 6a shows the size distribution of SAP A particles, where a size range from tens of microns to over 200 μm is evident. Ground SAP particles were

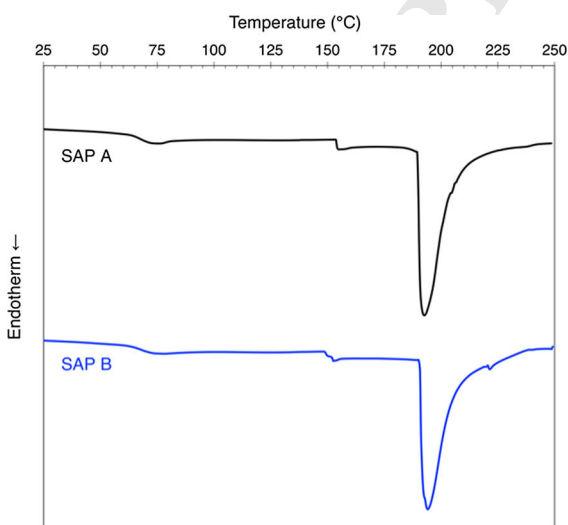


Fig. 4 DSC thermograms of biobased SAP samples



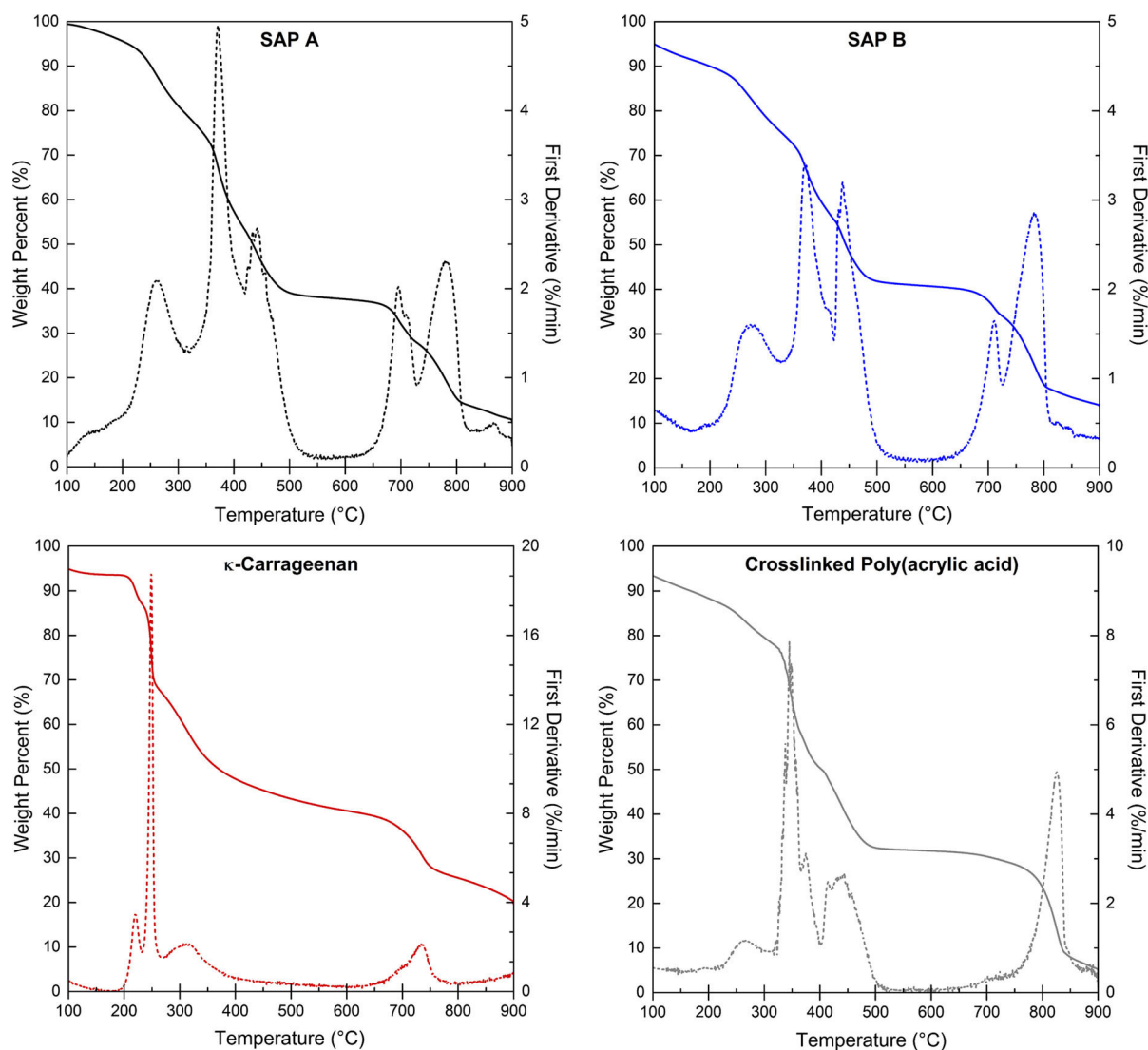


Fig. 5 TGA traces (solid line) with the accompanying first derivative (dashed line), reported in wt%/min, for the two SAPs (top) and the constituent materials (bottom)

389 passed through sieves ranging from 125 to 250 μm and
 390 a random sample of SAP was obtained to limit the
 391 particle size distribution before SEM imaging. Figure
 392 6b highlights a single SAP particle in the size
 393 range of 90 $\mu\text{m} \times 50 \mu\text{m}$. As expected, the particles
 394 exhibit an irregular shape, which can be attributed to
 395 manual grinding. This irregular morphology is similar
 396 to previously synthesized SAPs [29].

3.5 FTIR

The FTIR spectra for pure κC (red) and crosslinked
 poly(acrylic acid) (gray), as well as SAP A (black) and
 SAP B (blue), are shown in Fig. 7. The major peaks for
 each of the constituent materials are labeled in the
 color of the respective spectrums to indicate origin of
 the functional group signal in each SAP.

In the κC spectrum, signals at 1220, 1032, 922, and
 841 cm^{-1} correspond to the S=O stretch of sulfate
 esters, the C–O stretch of the glycosidic linkage, the
 C–O stretch of the 3,6-anhydro-D-galactose, and the

Fig. 6 SEM micrographs of biobased SAP confirming **a** $a < 200 \mu\text{m}$ particle size and **b** irregular particle morphology

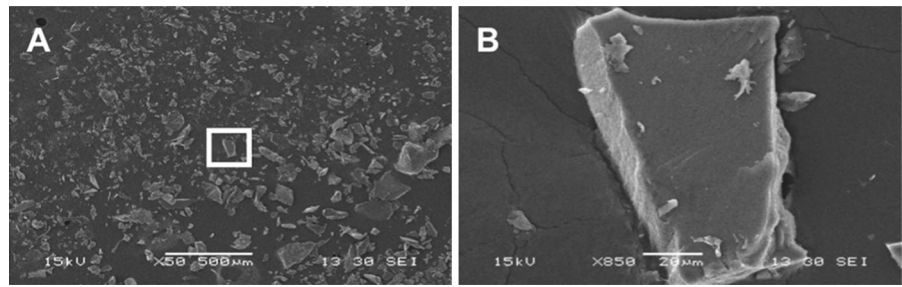
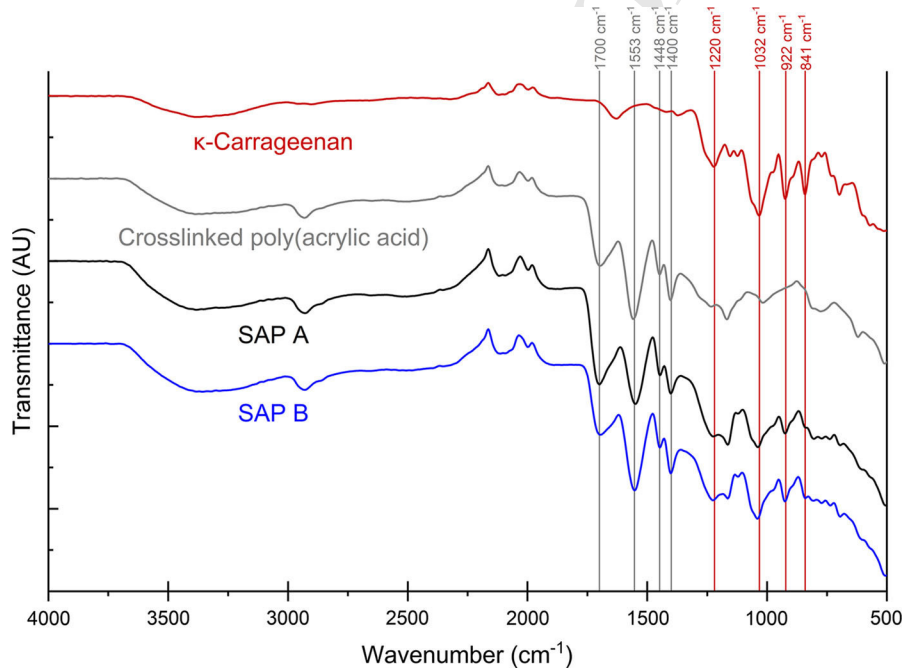


Fig. 7 The FTIR spectra for the two biobased SAPs (blue and black) and the constituent materials, κC (red) and crosslinked poly(acrylic acid) (gray)



408 C–O–S stretch of the D-galactose-4-sulfate, respec-
 409 tively [40]. In the crosslinked poly(acrylic acid)
 410 spectrum, signals at 1700, 1553, 1448, and
 411 1400 cm^{-1} correspond to the C=O stretch of the
 412 carbonyl, the COO^- stretching of the antisymmetric
 413 carboxylate ion, the CH_2 stretch of the backbone, and
 414 the COO^- stretching of the symmetric carboxylate
 415 ion, respectively [41]. Since the poly(acrylic acid) and
 416 SAPs were partially neutralized with NaOH in the
 417 synthesis process, the presence of carboxylic acid and
 418 carboxylate ions are observed in the IR spectra. These
 419 spectra indicate successful synthesis of a copolymer
 420 from κC and AA by showing that the characteristic
 421 signals for each material are carried through into the
 422 resulting SAPs.

3.6 Fresh-state properties

423
 424 As anticipated, the addition of SAP water to cement
 425 paste influenced set time and paste workability. The
 426 control paste set in 5.7 h, while the set times of cement
 427 pastes containing SAP A and SAP B—6.7 and 7.0 h,
 428 respectively—were delayed, as expected [31]. The
 429 workability of the cement pastes was reduced in
 430 samples that contained SAP A and SAP B. Modified
 431 miniature slump cone measurements for all samples
 432 were 12.5 mm for the control, and 2 and 7 mm for
 433 SAP A and SAP B, respectively. The paste spread did
 434 not change, and the paste was not flowable due to the
 435 low w/c ratio and a lack of superplasticizer.



Author Proof

436 3.7 Autogenous shrinkage

437 Figure 8 shows the results from the 28-day autogenous
 438 shrinkage tests for all cement paste samples that
 439 include SAP A and SAP B, as well as the control
 440 sample. Measurements commenced immediately after
 441 final time of set starting at Day 0. All paste samples
 442 exhibit an increase in positive strain immediately after
 443 final set (Fig. 8). After the first 24 h, however, the
 444 control sample experienced negative strain, while all
 445 samples containing the biobased SAPs experienced
 446 positive strain for the duration of the test. Negative
 447 strain indicates that the control sample was undergo-
 448 ing continuous self-desiccation. The control paste
 449 experienced a negative strain of -0.99 mm/m during
 450 the first 7 days. Positive strain observed in all cement
 451 paste samples containing the biobased SAPs show
 452 continuous expansion of the hardened paste for the
 453 first 7 days. The paste sample containing SAP A
 454 exhibited a maximum positive strain of 1.74 mm/m on
 455 day seven of the autogenous shrinkage test. The paste
 456 containing SAP B demonstrated the highest positive
 457 strain of 2.4 mm/m 7 days after final set. The control
 458 paste continued self-desiccation through 14 days at
 459 which time the sample developed a shrinkage crack
 460 (Fig. 8).

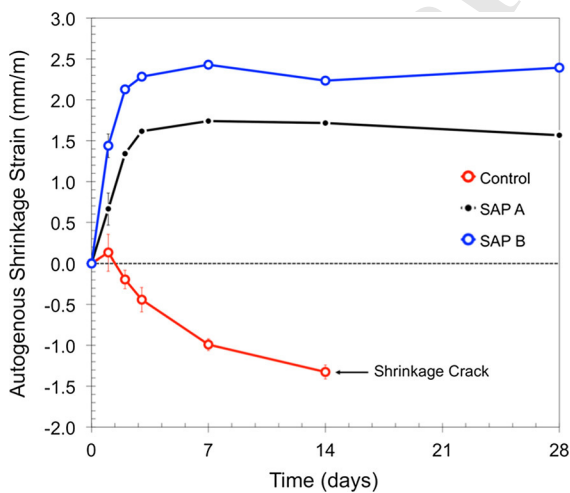


Fig. 8 Autogenous shrinkage strain measurements for control and SAP-containing cement pastes. Error bars represent \pm one standard deviation

4 Discussion 461

462 Two biobased SAPs from κ C with varying AA content 462
 463 were synthesized using ambient-condition free radical 463
 464 polymerization. The variation in AA was used to 464
 465 determine the swelling capability of the SAP based on 465
 466 the κ C backbone. From these data, the concentration 466
 467 of AA does not appear to influence SAP absorption in 467
 468 synthetic pore solution (Fig. 3), indicating that, even 468
 469 at lower AA concentrations, the biobased SAPs will 469
 470 absorb high amounts of ionic solution. These findings 470
 471 suggest that the natural swelling ability of the κ C, due 471
 472 to its intrinsic hydrophilicity, could be responsible for 472
 473 the swelling capacity of the biobased SAPs in pore 473
 474 solution. This result is an advantage of a biobased 474
 475 SAP, where, even with minimal AA concentrations, 475
 476 the κ C will allow for absorption and desorption of 476
 477 ionic fluid. 477

478 As shown in Fig. 3, the swelling behavior of the 478
 479 SAPs in pure water versus the NaOH solution also 479
 480 indicate that monovalent cations have an effect on the 480
 481 swelling ratio but not to the extent of the pore solution 481
 482 which contains mono and divalent cations (Na^+ , K^+ , 482
 483 Ca^{2+}). Previous studies have also observed a decrease 483
 484 in swelling capacity of SAPs in the presence of these 484
 485 cations due to their electrostatic attraction to the 485
 486 anionic functional groups within the polymer network 486
 487 [10, 42, 43]. More specifically, the carboxylate groups 487
 488 present in the SAPs are able to form an ionic complex- 488
 489 ation with the Ca^{2+} cations, thus creating a stable poly- 489
 490 mer network and lessening the absorption capacity of 490
 491 the SAP [42, 44]. 491

492 The swelling behavior of the SAPs in the NaOH and 492
 493 synthetic pore solutions indicate that the ion type and 493
 494 concentration has an effect on swelling capabilities. 494
 495 Even with exposure to cations (i.e., Na^+ , K^+ , Ca^{2+}), 495
 496 the ability of the SAP to swell in ionic solutions is 496
 497 evident. However, the fluctuation in swelling behavior 497
 498 in the synthetic pore solution for all samples indicates 498
 499 competition between cations and the polymer's affini- 499
 500 ty to uptake water, which provides clues to the 500
 501 swelling kinetics of the SAP in highly alkaline 501
 502 environments. While the absorption of the NaOH 502
 503 and pore solution is decreased compared to the 503
 504 aqueous solutions, the SAPs absorb ≥ 94 [g/g] of 504
 505 their original weight. This good absorption may be 505
 506 attributed to the ability of κ C to form gels, even in the 506
 507 presence of K^+ and Ca^{2+} ions [19, 45, 46]. 507



Author Proof

508 Thermal characterization, namely DSC and TGA,
 509 was used to verify that the biobased SAPs intended for
 510 use in cement-based mixtures were stable enough to
 511 handle the heat of hydration generated during curing
 512 without substantial thermal degradation. DSC analysis
 513 elucidated that the biobased SAPs can maintain
 514 functionality at temperatures up to 200 °C. TGA
 515 confirms this behavior in functionality, as it is noted
 516 that the SAP maintains > 90% of its original weight up
 517 to 200 °C.

518 SEM images of biobased SAP particle morphology
 519 reveled irregular particle shapes and sizes, which was
 520 to be expected based on previous studies and types of
 521 SAP polymerization techniques [11, 12, 29]. Particle
 522 size distribution before sieving ranged from a few
 523 microns to over 200 microns. For this study, the effect
 524 of particle shape was not considered. Other studies
 525 have shown that SAP particle size affects the rate of
 526 absorption and maximum absorption capacity and that
 527 spherical shapes may be most effective [47] at
 528 mitigating autogenous shrinkage in cement pastes,
 529 mortars, and concrete. Researchers have also sug-
 530 gested that spherical shapes may promote the devel-
 531 opment of more preferred capillary pore structures
 532 [22], although care must be taken to control particle
 533 size, since the swelling capacities of SAPs have been
 534 shown to increase non-linearly as the diameter of the
 535 SAP particle is increased [47]. Thus, while mechanical
 536 alteration of the shape of the biobased SAP could be
 537 further investigated to achieve more consistent parti-
 538 cle aspect ratios, careful control of diameter is critical
 539 to achieving maximum effectiveness.

540 Results of the autogenous shrinkage testing show
 541 that the addition of biobased SAP leads to a reduction
 542 in shrinkage to the point of net-positive expansion for
 543 both samples containing biobased SAP. The reference
 544 control sample exhibited a slight expansion during the
 545 initial measurements directly after the time of final set,
 546 which could be attributed to an initially high porosity
 547 that would reduce any self-desiccation stresses result-
 548 ing from continuous hydration. Figure 3 illustrates
 549 that the swelling behavior of both SAP A and SAP B in
 550 the synthetic pore solution plateaued after 10 min,
 551 quickly absorbing and retaining water that is available
 552 for cement hydration.

553 The high expansion values of cement pastes
 554 containing SAP A and B are higher than other
 555 expansion values reported in literature, where expan-
 556 sion of 1–2 (mm/m) strain is expected [31]. Snoeck

et al. [1] reports 0.2 (mm/m) strain reduction for SAP 557
 addition of 0.22% and Jensen et al. [31] observed 0.5 558
 (mm/m) strain for 0.3% SAP addition to cement paste. 559
 These lower values for expansion could be attributed 560
 to the utilization of additional admixtures. The cement 561
 pastes herein do not utilize any other admixtures (i.e., 562
 superplasticizers) or silica fume, since both of which 563
 exacerbates the water demand in cement pastes, 564
 mortars, and concrete, which in turn will cause a 565
 reduction in available water for the SAP to absorb. The 566
 studies referenced herein [1, 2, 48] report the use of 567
 carboxylate superplasticizers. Though proprietary, the 568
 chemical structure of the superplasticizers is similar to 569
 acrylic/acrylamide based SAPs, through the carboxy- 570
 late moieties. There is the potential for competition 571
 between the SAPs and the superplasticizers for water 572
 absorption, if these two chemicals are used in 573
 conjunction. The carboxylate moieties in the SAPs 574
 will be sterically hindered, due to the crosslinking, 575
 thus they will be less able to absorb water. To date the 576
 authors do not know of a study that reports the effects 577
 of superplasticizers or silica fume on the swelling 578
 kinetics of SAPs. Therefore, in the pure paste and 579
 SAP-containing samples, the authors would expect 580
 that the swelling ratios would be higher, leading to 581
 increased expansion values in the autogenous shrink- 582
 age testing. 583

584 Differences in autogenous shrinkage expansion
 585 values between SAP A and SAP B presented in this
 586 study could be attributed to the deswelling character-
 587 istics between the two SAPs in the presence of Ca²⁺
 588 cations. It has been previously discussed that the
 589 presence of divalent cations such as Ca²⁺ affects the
 590 swelling behavior of SAPs. Pourjavadi et al. [10] has
 591 reported on the deswelling of non-biobased SAPs in
 592 the presence of an artificial pore solution and a cement
 593 filtrate solution. The authors showed that, while the
 594 deswelling mechanisms are not well understood, the
 595 formation of calcium carbonate in the filtrate caused
 596 rapid deswelling due to the anionic groups in the SAP
 597 [10]. Krafcik et al. [29] also indicated that the
 598 magnitude of deswelling in ionic solutions is depen-
 599 dent on the amount of anionic groups and their
 600 interaction with Ca²⁺ ions. The increased amount of
 601 κC in SAP B would also act as a crosslinker due to the
 602 way in which the helical structures aggregate, causing
 603 the SAP to more rapidly release bound water. Thus,
 604 while the calcium ions may provide good swelling
 605 abilities of higher κC content gels, they may also play



606 a role in the de-swelling kinetics within paste, mortar,
607 and concrete.

608 Together, the swelling behavior (Fig. 3) and the
609 autogenous shrinkage data (Fig. 8) are indicative that
610 the biobased SAPs initially absorb and slowly release
611 ionic pore solution during cement hydration of low
612 w/c cement paste, effectively serving as an internal
613 curing agent and alleviating the deleterious effects of
614 autogenous shrinkage.

615 5 Conclusions

616 In this work, biobased superabsorbent polymers
617 (SAPs) derived from kappa-carrageenan (κ C) were
618 synthesized, and their swelling behavior was charac-
619 terized in tap water, deionized water, and synthetic
620 concrete pore solution. The effect of acrylic acid
621 monomer content on the swelling behavior was
622 explicitly investigated, as was the time to equilibrium
623 swelling. Results show that the ranges of equilibrium
624 swelling (~ 94 – 438 [g/g]) achieved by the biobased
625 SAPs investigated herein were on par with other
626 previously produced non-biobased synthetic SAPs and
627 that the biobased SAPs were successful in mitigating
628 autogenous shrinkage in a low water-to-cement (w/c)
629 ratio cement paste. While control cement paste
630 samples with no SAP exhibited early-age expansion
631 and eventual cracking due to self-desiccation, the
632 cement pastes containing 0.3% biobased SAPs by
633 weight of cement exhibited net-positive expansion.
634 Together, the swelling properties and autogenous
635 shrinkage results suggest that the SAPs created in this
636 work are promising biobased candidates for internal
637 curing agents that are used to improve early- and late-
638 age behavior of high-performance (i.e., low w/c)
639 cement pastes, mortars, and concrete.

640 **Acknowledgements** This research was made possible by the
641 Department of Civil, Environmental, and Architectural
642 Engineering, the College of Engineering and Applied
643 Sciences, and the Sustainable Infrastructure Materials
644 Laboratory (SIMLab) at the University of Colorado Boulder
645 with support from the from the National Science Foundation
646 (Award No. CMMI-1562557). The authors would like to thank
647 Shane Frazier for DSC data collection and Elizabeth Delesky for
648 data collection during time-of-set testing. This work represents
649 the views of the authors and not necessarily those of the
650 sponsors.

Funding This study was funded in part by the US National
Science Foundation (Award No. CMMI-1562557).

Compliance with ethical standards

Conflict of interest The authors declare that they have no
conflict of interest.

References

1. Snoeck D, Jensen OM, De Belie N (2015) The influence of superabsorbent polymers on the autogenous shrinkage properties of cement pastes with supplementary cementitious materials. *Cem Concr Res* 74:59–67. <https://doi.org/10.1016/j.cemconres.2015.03.020>
2. Mechtcherine V, Gorges M, Schroefl C, Assmann A, Brameshuber W, Ribeiro AB, Cusson D, Custódio J, Da Silva EF, Ichimiya K, Igarashi SI, Klemm A, Kovler K, De Mendonça Lopes AN, Lura P, Nguyen VT, Reinhardt HW, Filho RDT, Weiss J, Wyrzykowski M, Ye G, Zhutovsky S (2014) Effect of internal curing by using superabsorbent polymers (SAP) on autogenous shrinkage and other properties of a high-performance fine-grained concrete: results of a RILEM round-robin test. *Mater Struct Constr* 47:541–562. <https://doi.org/10.1617/s11527-013-0078-5>
3. Laustsen S, Hasholt MT, Jensen OM (2015) Void structure of concrete with superabsorbent polymers and its relation to frost resistance of concrete. *Mater Struct* 48:357–368. <https://doi.org/10.1617/s11527-013-0188-0>
4. Mönning S, Lura P (2007) Superabsorbent polymers—an additive to increase the freeze-thaw resistance of high strength concrete. *Adv Constr Mater* 351–358
5. Mechtcherine V, Schröfl C, Wyrzykowski M, Gorges M, Lura P, Cusson D, Margeson J, De Belie N, Snoeck D, Ichimiya K, Igarashi SI, Falikman V, Friedrich S, Bokern J, Kara P, Marciniak A, Reinhardt HW, Sippel S, Bettencourt Ribeiro A, Custódio J, Ye G, Dong H, Weiss J (2017) Effect of superabsorbent polymers (SAP) on the freeze–thaw resistance of concrete: results of a RILEM interlaboratory study. *Mater Struct Constr*. <https://doi.org/10.1617/s11527-016-0868-7>
6. Mignon A, Graulus GJ, Snoeck D, Martins J, De Belie N, Dubrue P, Van Vlierbergh S (2014) pH-sensitive superabsorbent polymers: a potential candidate material for self-healing concrete. *J Mater Sci* 50:970–979. <https://doi.org/10.1007/s10853-014-8657-6>
7. Snoeck D, Van Tittelboom K, Steuperaert S, Dubrue P, De Belie N (2014) Self-healing cementitious materials by the combination of microfibres and superabsorbent polymers. *J Intell Mater Syst Struct* 25:13–24. <https://doi.org/10.1177/1045389X12438623>
8. Zhu Q, Barney CW, Erk KA (2015) Effect of ionic crosslinking on the swelling and mechanical response of model superabsorbent polymer hydrogels for internally cured concrete. *Mater Struct* 48:2261–2276. <https://doi.org/10.1617/s11527-014-0308-5>



Author Proof

704 9. Zhang J, Wang Q, Wang A (2007) Synthesis and character- 765
 705 ization of chitosan-g-poly(acrylic acid)/attapulgitic 766
 706 superabsorbent composites. *Carbohydr Polym* 68:367–374. 767
 707 <https://doi.org/10.1016/j.carbpol.2006.11.018> 768
 708 10. Pourjavadi A, Fakoorpoor SM, Hosseini P, Khaloo A (2013) 769
 709 Interactions between superabsorbent polymers and cement- 770
 710 based composites incorporating colloidal silica nanoparti- 771
 711 cles. *Cem Concr Compos* 37:196–204. <https://doi.org/10.1016/j.cemconcomp.2012.10.005> 772
 712 11. Zohuriaan-Mehr MJ, Kabiri K (2008) Superabsorbent 773
 713 polymer materials, Iran. *Polym J* 17:451–477 774
 714 12. Ahmed EM (2015) Hydrogel: preparation, characterization, 775
 715 and applications: a review. *J Adv Res* 6:105–121. <https://doi.org/10.1016/j.jare.2013.07.006> 776
 716 13. Buchholz FL, Graham AT (1998) Modern superabsorbent 777
 717 polymer technology. Wiley-VCH, New York 778
 718 14. Feng E, Ma G, Wu Y, Wang H, Lei Z (2014) Preparation 779
 719 and properties of organic-inorganic composite superab- 780
 720 sorbent based on xanthan gum and loess. *Carbohydr Polym* 781
 721 111:463–468. <https://doi.org/10.1016/j.carbpol.2014.04.031> 782
 722 15. Bhardwaj TR, Kanwar M, Lal R, Gupta A (2000) Natural 783
 723 gums and modified natural gums as sustained-release carri- 784
 724 ers. *Drug Dev Ind Pharm* 26:1025–1038. <https://doi.org/10.1081/DDC-100100266> 785
 725 16. Manuhara GJ, Praseptianga D, Riyanto RA (2016) 786
 726 Extraction and characterization of refined K-carrageenan of 787
 727 red algae [*Kappaphycus alvarezii* (Doty ex P.C. Silva, 788
 728 1996)] originated from Karimun Jawa Islands. *Aquat Proce- 789*
 729 dia 7:106–111. <https://doi.org/10.1016/j.aqpro.2016.07.014> 790
 730 17. Rostamnia S, Doustkhah E, Baghban A, Zeynizadeh B 791
 731 (2016) Seaweed-derived κ-carrageenan: modified κ-car- 792
 732 rageenan as a recyclable green catalyst in the multicompo- 793
 733 nent synthesis of aminophosphonates and polyhydroquinolines. *J Appl Polym Sci* 133:1–7. <https://doi.org/10.1002/app.43190> 794
 734 18. Campo VL, Kawano DF, da Silva DB, Carvalho I (2009) 795
 735 Carrageenans: biological properties, chemical modifica- 796
 736 tions and structural analysis—a review. *Carbohydr Polym* 797
 737 77:167–180. <https://doi.org/10.1016/j.carbpol.2009.01.020> 798
 738 19. Chronakis IS, Piculell L, Borgström J (1996) Rheology of 799
 739 kappa-carrageenan in mixtures of sodium and cesium 800
 740 iodide: two types of gels. *Carbohydr Polym* 31:215–225. 801
 741 [https://doi.org/10.1016/S0144-8617\(96\)00117-8](https://doi.org/10.1016/S0144-8617(96)00117-8) 802
 742 20. Liu S, Li L (2016) Thermoreversible gelation and scaling 803
 743 behavior of Ca²⁺-induced κ-carrageenan hydrogels. *Food 804*
 744 Hydrocoll 61:793–800. <https://doi.org/10.1016/j.foodhyd.2016.07.003> 805
 745 21. Wang F, Zhou Y, Peng B, Liu Z, Hu S (2009) Autogenous 806
 746 shrinkage of concrete with super-absorbent polymer. *ACI 807*
 747 Mater J 106:123–127 808
 748 22. Jensen OM, Hansen PF (2001) Water-entrained cement- 809
 749 based materials—I. Principles and theoretical background. 810
 750 *Cem Concr Res* 31:647–654. [https://doi.org/10.1016/S0008-8846\(01\)00463-X](https://doi.org/10.1016/S0008-8846(01)00463-X) 811
 751 23. Bentur A, Igarashi SI, Kovler K (2001) Prevention of 812
 752 autogenous shrinkage in high-strength concrete by internal 813
 753 curing using wet lightweight aggregates. *Cem Concr Res* 814
 754 31:1587–1591. [https://doi.org/10.1016/S0008-8846\(01\)00608-1](https://doi.org/10.1016/S0008-8846(01)00608-1) 815
 755 24. Mechtcherine V, Reinhardt H-W (eds) (2012) Application 816
 756 of superabsorbent polymers (SAP) in concrete construction: 817
 757 state-of-the-art report prepared by Technical Committee 818
 758 225-SAP. <https://doi.org/10.1007/978-94-007-2733-5> 819
 759 25. Weber S, Reinhardt HW (1997) A new generation of high 820
 760 performance concrete: concrete with autogenous curing. 821
 761 *Adv Cem Based Mater* 6:59–68. [https://doi.org/10.1016/S1065-7355\(97\)00009-6](https://doi.org/10.1016/S1065-7355(97)00009-6) 822
 762 26. Mechtcherine V, Snoeck D, Schröfl C, De Belie N, Klemm 823
 763 AJ, Ichimiya K, Moon J, Wyrzykowski M, Lura P, Tor- 824
 764 opovs N, Assmann A, Igarashi S, De La Varga I, Almeida 825
 765 FCR, Erk K, Ribeiro AB, Custódio J, Reinhardt HW, 826
 766 Falikman V (2018) Testing superabsorbent polymer (SAP) 827
 767 sorption properties prior to implementation in concrete: 828
 768 results of a RILEM Round-Robin Test. *Mater Struct* 51:28. 829
 769 <https://doi.org/10.1617/s11527-018-1149-4> 830
 770 27. Schröfl C, Snoeck D, Mechtcherine V (2017) A review of 831
 771 characterisation methods for superabsorbent polymer (SAP) 832
 772 samples to be used in cement-based construction materials: 833
 773 report of the RILEM TC 260-RSC. *Mater Struct Constr.* 834
 774 <https://doi.org/10.1617/s11527-017-1060-4> 835
 775 28. Ghods P, Isgor OB, McRae G, Miller T (2009) The effect of 836
 776 concrete pore solution composition on the quality of passive 837
 777 oxide films on black steel reinforcement. *Cem Concr 838*
 778 Compos 31:2–11. <https://doi.org/10.1016/j.cemconcomp.2008.10.003> 839
 779 29. Krafcik MJ, Erk KA (2016) Characterization of superab- 840
 780 sorbent poly(sodium-acrylate acrylamide) hydrogels and 841
 781 influence of chemical structure on internally cured mortar. 842
 782 *Mater Struct* 49:4765–4778. <https://doi.org/10.1617/s11527-016-0823-7> 843
 783 30. Justs J, Wyrzykowski M, Winnefeld F, Bajare D, Lura P 844
 784 (2014) Influence of superabsorbent polymers on hydration 845
 785 of cement pastes with low water-to-binder ratio: a 846
 786 calorimetry study. *J Therm Anal Calorim* 115:425–432. 847
 787 <https://doi.org/10.1007/s10973-013-3359-x> 848
 788 31. Jensen OM, Hansen PF (2002) Water-entrained cement- 849
 789 based materials: II. Experimental observations. *Cem Concr 850*
 790 Res 32:973–978. [https://doi.org/10.1016/S0008-8846\(02\)00737-8](https://doi.org/10.1016/S0008-8846(02)00737-8) 851
 791 32. Kantro DL (1980) Influence of water-reducing admixtures 852
 792 on properties of cement paste—a miniature slump test. *Cem 853*
 793 Concr Aggreg. 2:95–102. doi: <http://dx.doi.org/10.1520/CCA10190J>. ISSN 0149-6123 854
 794 33. Pourjavadi A, Harzandi AM, Hosseinzadeh H (2004) 855
 795 Modified carrageenan 3. Synthesis of a novel polysaccha- 856
 796 ride-based superabsorbent hydrogel via graft copolymer- 857
 797 ization of acrylic acid onto kappa-carrageenan in air. *Eur 858*
 798 Polym J 40:1363–1370. <https://doi.org/10.1016/j.eurpolymj.2004.02.016> 859
 799 34. Eisenberg A, Yokoyama T (1969) Dehydration kinetics and 860
 800 glass transition of poly(acrylic acid). *J Polym Sci* 861
 801 7:1717–1728 862
 802 35. Mitsuiki M, Yamamoto Y, Mizuno A, Motoki M (1998) 863
 803 Glass transition properties as a function of water content for 864
 804 various low-moisture galactans. *J Agric Food Chem* 865
 805 46:3528–3534. <https://doi.org/10.1021/jf9709820> 866
 806 36. Blanshard JMV, Lillford P, Easter S (1993) School in 867
 807 agricultural science (53rd: 1992: Nottingham University), 868
 808 the glassy state in foods, Nottingham University Press. 869
 809 870
 810
 811
 812
 813
 814
 815
 816
 817
 818
 819
 820
 821
 822
 823
 824



- 825 [https://espace.library.uq.edu.au/view/UQ:236984#.](https://espace.library.uq.edu.au/view/UQ:236984#.WiBdrtx65fw.mendeley)
826 [WiBdrtx65fw.mendeley](https://espace.library.uq.edu.au/view/UQ:236984#.WiBdrtx65fw.mendeley). Accessed 30 Nov 2017
- 827 37. Frazier SD, Srubar WV (2016) Evaporation-based method
828 for preparing gelatin foams with aligned tubular pore
829 structures. *Mater Sci Eng C* 62:467–473. [https://doi.org/10.](https://doi.org/10.1016/j.msec.2016.01.074)
830 [1016/j.msec.2016.01.074](https://doi.org/10.1016/j.msec.2016.01.074)
- 831 38. Carrageenan (Red Seaweed), (n.d.). [http://www.](http://www.cargohandbook.com/index.php/Carrageenan_(Red_Seaweed))
832 [cargohandbook.com/index.php/Carrageenan_\(Red_](http://www.cargohandbook.com/index.php/Carrageenan_(Red_Seaweed))
833 [Seaweed\)](http://www.cargohandbook.com/index.php/Carrageenan_(Red_Seaweed)). Accessed 16 Nov 2017
- 834 **AQ6** 39. Shawe J, Riesen R, Widmann J, Schubnell M (2000)
835 UserCom, Mettler Toledo 1–28
- 836 40. Chopin T, Whalen E (1993) A new and rapid method for
837 carrageenan identification by FT IR diffuse reflectance
838 spectroscopy directly on dried, ground algal material. *Car-*
839 *bohydr Res* 246:51–59. [https://doi.org/10.1016/0008-](https://doi.org/10.1016/0008-6215(93)84023-Y)
840 [6215\(93\)84023-Y](https://doi.org/10.1016/0008-6215(93)84023-Y)
- 841 41. Kirwan LJ, Fawell PD, Van Bronswijk W (2003) In situ
842 FTIR-ATR examination of poly(acrylic acid) adsorbed onto
843 hematite at low pH. *Langmuir* 19:5802–5807. [https://doi.](https://doi.org/10.1021/la027012d)
844 [org/10.1021/la027012d](https://doi.org/10.1021/la027012d)
- 845 42. Schröfl C, Mechtcherine V, Gorges M (2012) Relation
846 between the molecular structure and the efficiency of
847 superabsorbent polymers (SAP) as concrete admixture to
848 mitigate autogenous shrinkage. *Cem Concr Res*
849 42:865–873. [https://doi.org/10.1016/j.cemconres.2012.03.](https://doi.org/10.1016/j.cemconres.2012.03.011)
850 [011](https://doi.org/10.1016/j.cemconres.2012.03.011)
43. Krafcik MJ, Macke ND, Erk KA (2017) Improved concrete
851 materials with hydrogel-based internal curing agents. *Gels*
852 3:46. <https://doi.org/10.3390/gels3040046>
853
44. Plank J, Sachsenhauser B (2009) Experimental determina-
854 tion of the effective anionic charge density of polycar-
855 boxylate superplasticizers in cement pore solution. *Cem*
856 *Concr Res* 39:1–5. [https://doi.org/10.1016/j.cemconres.](https://doi.org/10.1016/j.cemconres.2008.09.001)
857 [2008.09.001](https://doi.org/10.1016/j.cemconres.2008.09.001)
45. Therkelsen GH, Carrageenan (1993) In: Whistler RL,
858 BeMiller JN (eds) *Industrial gums: polysaccharides and*
859 *their derivatives*, pp 146–176
46. Kara S, Tamerler C, Pekcan Ö (2003) Cation effects on
860 swelling of κ -carrageenan: a photon transmission study.
861 *Biopolymers* 70:240–251. [https://doi.org/10.1002/bip.](https://doi.org/10.1002/bip.10467)
862 [10467](https://doi.org/10.1002/bip.10467)
47. Esteves LP (2011) Superabsorbent polymers: on their
863 interaction with water and pore fluid. *Cem Concr Compos*
864 33:717–724. [https://doi.org/10.1016/j.cemconcomp.2011.](https://doi.org/10.1016/j.cemconcomp.2011.04.006)
865 [04.006](https://doi.org/10.1016/j.cemconcomp.2011.04.006)
48. Justs J, Wyrzykowski M, Bajare D, Lura P (2015) Internal
866 curing by superabsorbent polymers in ultra-high perfor-
867 mance concrete. *Cem Concr Res* 76:82–90. <https://doi.org/10.1016/j.cemconres.2015.05.005>
868
869
870
871
872
873

UNCORRECTED